J Clin Periodontol 2011; 38: 1130–1136 doi: 10.1111/j.1600-051X.2011.01790.x

Journal of Clinical Periodontology

Engineering of a periodontal ligament construct: cell and fibre alignment induced by shear stress

Sahng G. Kim[1,2], Seong-Gon Kim[2,3], Bryon Viechnicki[2], Syngcuk Kim[1] and Hyun-Duck Nah[2,4]

[1]Department of Endodontics, School of Dental Medicine, University of Pennyslvania, Philadelphia, PA, USA; [2]Division of Plastic and Reconstructive Surgery, The Children's Hospital of Philadelphia, Philadelphia, PA, USA; [3]Department of Oral and Maxillofacial Surgery, College of Dentistry, Gangneung-Wonju National University, Gangneung, Gangwon, Korea; [4]Division of Plastic Surgery, Department of Surgery, School of Medicine, University of Pennsylvania, Philadelphia, PA, USA

Kim SG, Kim S-G, Viechnicki B, Kim S, Nah H-D, Engineering of a periodontal ligament construct: cell and fibre alignment induced by shear stress. J Clin Periodontol 2011; 38: 1130–1136. doi: 10.1111/j.1600-051X.2011.01790.x.

Abstract

Aim: We report an *in vitro* technique to establish alignment of collagen fibres and cells within a three-dimensional tissue equivalent that mimics the natural periodontal ligament (PDL) using a novel custom-designed bioreactor.

Material and Methods: Shear stress was applied to the tissue equivalent prepared with collagen solution and seeded with human PDL cells. Stress-strain dynamics and the alignment of collagen fibres and PDL cells in tissue equivalents were analysed.

Results: Shear stress aligned collagen fibres and PDL cells in a direction parallel to the principle strain vector. PDL cells and Collagen fibres aligned in strained tissue equivalents with higher uniformity than in unstrained tissue equivalents.

Conclusions: The cell and fibre alignment of the engineered PDL was precisely guided by mechanical shear stress along the direction of principal strain vector using a custom-designed bioreactor, suggesting that the enhanced functional property of engineered PDL constructs could be achieved with this technique.

Key words: alignment; collagen fibres; periodontal ligament; shear stress; tissue engineering

Accepted for publication 16 August 2011

The periodontal ligament (PDL), which attaches the two distinct types of hard tissues – cementum and bone, mainly consists of collagen fibres and heterogeneous cell populations of fibroblasts, cementoblasts, osteoblasts, osteoclasts and their progenitors. The PDL fibres are organized perpendicular to the tooth surface, and their ends are embedded in cementum and alveolar bone, forming Sharpey's fibres. Such arrangements keep the structural integrity of the periodontium and distribute masticatory forces on the tooth to the contiguous alveolar bone. In addition, the unique alignment of the PDL fibres is essential for alveolar bone growth in children as well as orthodontic tooth movement (Cronin et al. 1994, Henneman et al. 2008). Without a PDL, the tooth is ankylosed and bone growth arrested (Beertsen et al. 1997).

Biogenesis of a PDL with proper functional orientation remains as a challenge despite being an active area of research. Over the years, numerous attempts have been made to develop the PDL around cementum/root surfaces (Young et al. 2005, Flores et al. 2008) and dental implants (Bernstein et al. 1988, Preisig & Schroeder 1988, Buser et al. 1990, Warrer et al. 1993, Choi 2000, Gray & Vernino 2004, Parlar et al. 2005, Gault et al. 2010). However, new PDL regeneration with functional orientation was observed in a few studies (Flores et al. 2008, Gault et al. 2010), whereas most of studies showed connective tissue encapsulation or random collagen fibre alignment in newly regenerated PDL-like tissues.

Conflict of interest and source of funding statement

The authors declare that they have no conflict of interests.

This work was supported by the Academic Development Fund from the Children's Hospital of Philadelphia awarded to H.-D.N.

The growth and development of our bodies and the necessary lifelong tissue remodelling may not be achieved without an adequate type and amount of mechanical signals. It has been shown that physiological mechanical stress sustains the PDL *in vivo* and that several modalities of mechanical stress can cause alignment of cell-seeded tissue equivalents *in vitro*. Mechanical stress below physiological level, i.e. hypofunction, causes narrowing and disorganization of PDL structures (Cohn 1966, Levy & Mailland 1980, Beertsen 1987). For the tissues that are repeatedly challenged by specific types of stress under physiological conditions, a number of studies have incorporated tissue-specific mechanical forces in their strategies to achieve functional competency of the final tissue constructs. For example, compressive stress was used to enhance the functional property of an engineered cartilage construct (Waldman et al. 2004). Similarly, tensional stress was used for an engineered cardiac graft (Akhyari et al. 2002) and pulsatile stress for a blood vessel construct (Niklason et al. 1999).

A PDL tissue construct can be engineered *in vitro* with a mechanical shear stress to enhance its functional competency because the major type of mechanical stress that PDL is subjected to is shear stress. Therefore, the purpose of this study is to reproduce the functional alignment of collagen fibres and cells of the natural PDL by applying shear stress to a three-dimensional tissue equivalent seeded with PDL cells. We also quantitatively analyse the alignment of PDL cells and collagen fibres in the tissue equivalent, because the effect of shear stress on the alignment remains poorly understood. We report an *in vitro* technique to establish alignment of collagen fibres and cells within a three-dimensional tissue equivalent that mimics the natural PDL using a novel custom-designed bioreactor.

Material and Methods

Cell culture

Human PDL cells (provided by Dr. Shi at University of Southern California) isolated as previously described (Seo et al. 2004) were cultured in α-minimum essential medium (α-MEM; GIBCO/BRL, Grand Island, NY, USA) supplemented with 100 μg/ml streptomycin (GIBCO/BRL), 100 IU/ml penicillin (GIBCO/BRL) and 2.5 μg/ml amphotericin B (Fungizone; GIBCO/BRL) containing 15% fetal bovine serum (FBS; Atlanta Biologicals, Lawrenceville, GA, USA) in a humidified atmosphere of 5% CO_2 at 37°C.

For GFP (green fluorescent protein) transfection, PDL cells were cultured, trypsinized and plated at 1×10^5 cells in 2 ml media per well in six-well plates (Corning Incorporated, Corning, NY, USA) in serum-free minimum essential medium (MEM; GIBCO/BRL) without supplements. PDL cells were transfected with 20 μl of diluted eGFP plasmid DNA (0.15 μg/μl) using FuGENE® 6 Transfection Reagent (Roche Applied Science, Mannheim, Germany).

Three-dimensional tissue equivalent

Sterile acid-soluble rat-tail collagen type I (3.64 mg/ml; BD Sciences, Bedford, MA, USA) was mixed with 0.2 ml of 10× MEM (GIBCO/BRL) and 8 μl of antibiotics and antimycotic mix (100 μg/ml streptomycin, 100 IU/ml penicillin and 2.5 μg/ml amphotericin B) and 325 μl of acetic acid (Fisher Scientific, Ann Arbor, MI, USA). The solution was neutralized with 15 μl of 0.1N sodium hydroxide (Fisher Scientific). PDL cells (1.4×10^6 cells/ml) were added to the collagen solution to prepare 3×10^5 cells/ml of collagen solution in final concentration of 1.98 mg/ml. The collagen-cell mixture was incubated at 37°C in a humidified atmosphere of 5% CO_2 for about 45 min. until it became a gel. All the prior steps were done on ice.

Custom designed bioreactor

The bioreactor has three main parts comprising the infusion pump, the shear stress device and the connecting tube (Fig. 1A). The infusion pump functions as a source of mechanical energy by injecting fluid through a syringe. The shear stress device comprises a glass syringe, a shank and the shear stress system (Fig. 1B). The linear fluid movement in the syringe is converted to the linear mechanical movement of the piston. This force is transmitted by the shank to the shear stress system. The shear stress system is where this linear mechanical movement of the piston is transformed into the shear stress (Fig. 1C). The shank is composed of a glass piston, a stainless steel connector, and a Teflon® guiding plate and a brass clamp holder (Fig. 1D). In the shear stress system (Fig. 1C,D), cells are cultured in a three-dimensional collagen gel and shear stress is applied to the cells and fibres in this cell culture system. All parts of the device were autoclavable without any deformation. Shear strain was applied to the collagen gel by moving one of two parallel titanium mesh plates in the culture chamber 2 mm at a rate of 0.5 mm/h.

Computerized simulation of shear stress system with finite element method

The finite element analysis was carried out with ANSYS Workbench 10.0 (ANSYS, Inc., Canonsburg, PA, USA) to understand the shear stress-strain dynamics of the collagen gel in the bioreactor. A finite element model was created based on the following assumptions. The three-dimensional model has the same dimensions as the collagen gel in the experiment, which is $15 \times 4 \times 1$ mm^3 (length × width × depth, measured in mm each) in size. The mechanical properties of collagen gel were determined based on the value of the neohookean solid. The linear modulus (16.6 kPa) for a typical collagen gel was taken from Roeder et al. (2004). The shear modulus for the collagen gel (97 ± 4) was determined using a parallel plate rheometer (TA instruments RFS II). The incompressibility was assumed to be that of water.

Microscopy

An inverted microscope with digital camera (Olympus DP70, Olympus America, Melville, NJ, USA) was used for image acquisition of cells inside the gel. For fibre alignment analysis, the samples were fixed in a Karnovsky solution for an hour, processed for scanning electron microscopy (SEM), and examined under a JEOL JSM-T330A microscope at 15 kV, as previously described (Hillmann et al. 1999).

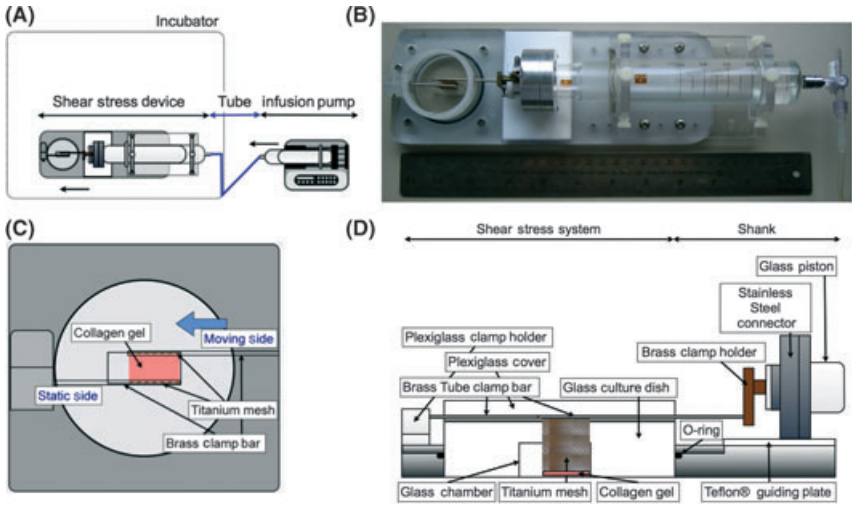

Fig. 1. Custom-designed bioreactor. (A) Schematic of experimental setup. The arrow shows the transmission of force from the infusion syringe pump to the shear stress device through the connecting tube. The system is designed to have the experiments performed inside an incubator. The infusion pump precisely controls a rate of fluid flow with a 1600/sec maximum step rate and 18 kg of linear force. (B) Mechanical shear stress device comprising a 50 ml glass syringe, a shank and a shear stress system. A glass syringe (50 ml BD Yale™ glass syringe; Becton-Dickinson & Co., Franklin Lakes, NJ, USA) is incorporated into the design of the device to receive the fluid being injected by the infusion syringe pump. The glass material allows the piston to slide with a constant rate reflecting the rate of infusion pump. (C) Schematic (top view) of the shear stress system illustrating the moving side and static side of the brass clamp bar. The arrow shows the movement of the titanium mesh of the moving side clamp bar. The shear stress is exerted in the gel during the movement of a titanium mesh on the moving clamp bar. (D) Schematic (side view) of the shear stress device showing the shank and the shear stress system. The flat bottom of the stainless steel connector is designed to sit on the Teflon® guiding plate, thus allowing the connector-holding glass piston to slide without rotating. The brass clamp holder connects the shank to the shear stress system. Two parallel titanium meshes are held by the clamp bar. The clamp bar is nickel plated to prevent the corrosion of the brass. The titanium meshes are placed in the glass chamber in the centre of glass culture dish. The titanium meshes are chosen to ensure the greater attachment of the collagen gel, minimizing detachment of the gel under shear stress. The collagen gels, seeded with and without cells with dimensions of $15 \times 4 \times 1$ mm^3 (length × width × depth, measured in mm each), are poured between the two titanium meshes. A plexiglass cover is used to prevent the possibility of contamination during the experiment inside of an incubator. To get a clear image of GFP-transfected PDL cells under the inverted light microscope, a quartz glass plate is used as a base to the glass culture dish. The culture dish is held by a rubber O-ring in the platform allowing the dish to be taken out with ease for sample preparation for scanning electron microscopy. The cells and fibres in the collagen gel experience shear stress during the movement of the titanium mesh. The static shear stress is applied to the gel for 24 h, immediately after the collagen-cell mixture became a gel. Shear strain is applied to the collagen gel by moving one of two parallel titanium mesh plates in the culture chamber 2 mm at a rate of 0.5 mm/h.

Estimation of shear stress in a three-dimensional collagen

To estimate the shear stress in the shear stress system, the rheology test of a collagen gel was carried out with ARES rheometer (Rheometric Scientific Ltd., Piscataway, NJ, USA). The collagen gel was loaded on a rotating plate under the geometry of the cone and plate, and its viscosity was measured. The shear stress, τ, is a function of the shear rate, γ, and viscosity, η, of the scaffold material.

$$\tau = \gamma \times \eta \qquad (1)$$

Analyses for PDL cell and collagen fibre alignment

For analysis of cell alignment, the angles of the long axis of each cell (θ) over two experimental time periods were measured manually to calculate the mean angle (θ mean) and angular standard deviation (σ). The data sets include the initial angle of cell orientation and the angle 24 h after the 2 mm movement of the titanium mesh. These values were calculated using circular statistics (Wagenseil et al. 2004).

For the analysis of collagen fibre alignment, an imaging module of Continuity 6.3 (Cardiac Mechanics Research Group, University of California San Diego) was used to measure the angles of the collagen fibres and to calculate θ mean and σ of the collagen fibres. The Fast Fourier transform (FFT) algorithm was used with image processing software Image-Pro Plus (MediaCybernetics, Bethesda, MD, USA) to show spatial distribution of collagen fibres. Watson–Wheeler *F*-test using circular statistics software Oriana 2.0 (Kovach Computing Services, Anglesey, Wales, UK) was performed to test whether or not each of the two angular data sets were significantly different from each other in mean angle and angular standard deviation.

Strain measurement in shear stress system

Acrylic powder markers (Jet Tooth Shade Powder; Lang Dental Mfg CO., Wheeling, IL, USA) were incorporated into a collagen gel and the locations of the markers were tracked using a digital camera with 4 mega pixel resolution and 38 mm lens (Canon SD10) to calculate the principal strain.

Results

Stress distribution in a three-dimensional tissue equivalent

Equivalent stress, i.e. Von-Mises Stress was used in the finite element analysis, which is defined as the sum of the squares of the three principal components (*x, y* and *z* axis) of the stress at a point in a three-dimensional model. Equivalent stress is a scalar value and only provides the magnitude without direction. It is useful when analysing a three-dimensional model to determine the stress distribution and visualize the plastic deformation. The centre of the gel

had almost homogenous stress distribution throughout the entire thickness, whereas the free borders on the top and bottom have isolated distribution of smaller stress (Fig. 2).

Shear stress estimation in a three-dimensional tissue construct

The shear stress was calculated from the equation (1). Figure 3 shows the results of shear stress calculated from the viscosity. The shear stress remained relatively constant in the range of the specific shear rates without build-up. This type of material is called "yield stress" material. In our experiments, we may expect that the collagen gel does not start to flow without a certain amount of stress. As the shear rate increased, the viscosity increases in the range of lower shear rate, approximately between 10^{-4} and 5×10^{-4} [s^{-1}]. It may show a plateau and be considered as zero shear viscosity, which is defined as the viscosity of a material when it is undisturbed. It may be reasonable to take the shear stress value from the range of constant shear stresses calculated from data in the range of shear rate 10^{-3} to 10^{-1} [s^{-1}], where it is 1.358537 ± 0.534296 [Pa] (Mean ± SD).

Shear stress-induced PDL cell alignment

The orientation of the cell changed with the amount of movement of the titanium mesh (Fig. 4A). Most of the PDL cells that were subjected to 24-h shear stress became more aligned in the direction of the strain, compared to the orientation of the control group (Fig. 4B). In addition, these cells in the experimental group became bipolar in shape (Fig. 4Ca, Cb). The cells in the experimental group that were initially oriented perpendicular to the strain became more rounded (Fig. 4Cc).

Circular statistics were used to investigate if there was any significant change in angular data before and after stress was applied. Initially, θ mean was 120°, and σ was 45°. Twenty four hours after shear stress was applied, θ mean was 57°, and σ was 37°. Watson–Wheeler *F*-test showed that the two angular data sets were significantly different ($p = 2.18 \times 10^{-4}$).

Shear stress-induced collagen fibre alignment

Collagen fibres that were randomly situated when no force was applied became aligned in the three-dimensional collagen gel when shear stress was applied (Fig. 5a). The FFT output images showed that under stress condition, pixels were distributed in an elliptical shape, indicating that the fibres were preferentially distributed in the direction connecting the top right to bottom left. On the other hand, under no stress condition, the frequency pattern was fairly spherical in shape, indicating that fibres were randomly distributed (Fig. 5B).

The normalized frequencies of the angles of fibres were plotted to determine orientation of collagen fibres (Fig. 5C). In the strained cell-seeded collagen gel, θ mean was 59°, and σ was 21°. In the unstrained cell-seeded collagen gel, θ mean was 80°, and σ was 69°. In the strained unseeded collagen gel, θ mean was 40°, and σ was 15°. In the unstrained unseeded collagen gel, θ mean was 88°, and σ was 75°. Watson–Wheeler *F*-test showed that any two angular data were significantly different ($p < 1 \times 10^{-12}$).

Correlation of cell and fibre alignment with principal strain vector

The principle strain vector was calculated with the method illustrated (Fig. 6A). θ mean of PDL cell and collagen fibre alignment was compared to that of the principal strain in the shear stress system. The principal strain was calculated to have a magnitude of 0.1 ± 0.09 with 60°

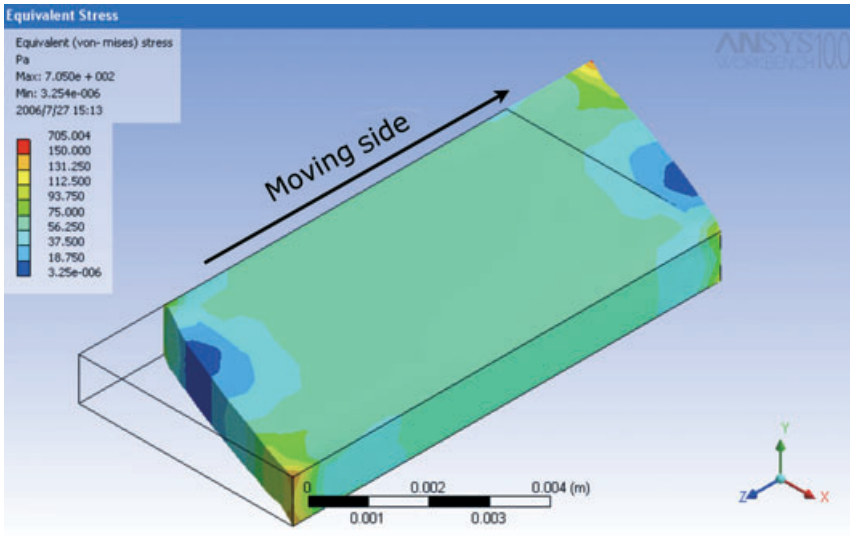

Fig. 2. Perspective view of equivalent (von-Mises) stress distribution in a three-dimensional collagen gel. The centre of the gel had almost homogenous stress distribution throughout the entire thickness, whereas the free borders on the top and bottom have isolated distribution of smaller stress. The stress distribution was visualized by a colour gamut ranging from red to blue. The highest stress was represented with red, and lowest stress with blue. Note that the edge between the two titanium meshes is not perfectly straight and the smaller stress distribution is lower in the centre of the free border.

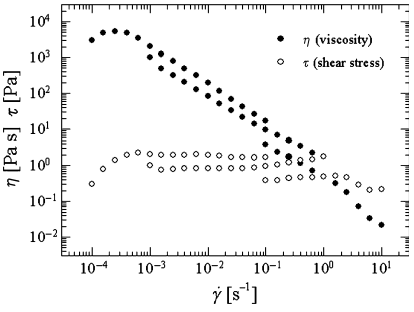

Fig. 3. The viscosity (η) and shear stress (τ) calculated by rheology test. The collagen gel is a non-Newtonian type fluid-like material with high viscosity and nonlinearity. In other words, the viscosity varies with the shear rate (γ). The shear stress remained relatively constant in the range of the specific shear rates without build-up. This type of material is called "yield stress" material. Toothpaste is one such material. It will start to flow out from the tube after a certain period of time of squeezing.

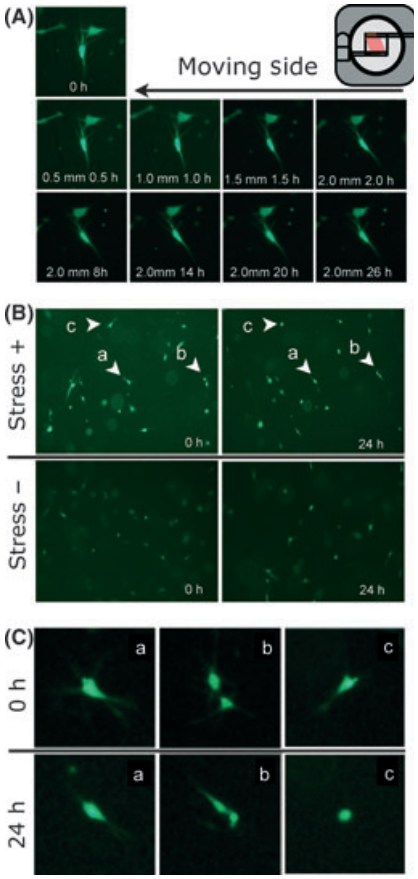

Fig. 4. Alignment of PDL cells. (A) Orientations of a PDL cell under shear stress in the three-dimensional tissue equivalent, before shear stress, after 0.5 (0.5 h), 1.0 (1.0 h), 1.5 (1.5 h), 2.0 (2.0 h) mm of titanium mesh movement, and 8, 14, 20, 26 h segments after shear stress. (B) PDL cell alignment in the three-dimensional tissue equivalent, before stress, 24 h after stress, in the experimental group (Stress +), and at initial state, 24 h, in control (Stress −). (C) The morphology and orientation of the cells in Figure 2B (a, b, and c) before stress and after 24 h.

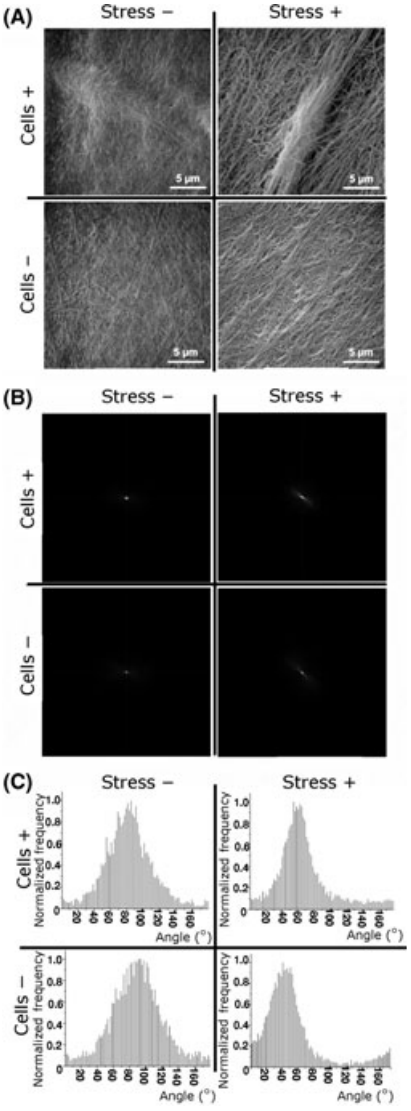

Fig. 5. Alignment of collagen fibres. (A) SEM micrographs of alignment of collagen fibres in three-dimensional tissue equivalent, seeded with or without PDL cells, with or without shear stress. Note the PDL cells were covered by collagen fibres (Magnification: 1500×, JEOL JSM-T330A). (B) FFT (Fast Fourier Transform) output images of Figure 5A. (C) Normalized frequency plots against angle of fibre orientation in strained cell-seeded, unstrained cell-seeded, strained cell-unseeded, and unstrained cell-unseeded tissue equivalents. Note the narrower distribution of angles of fibre orientation in the strained tissue equivalent (right column) compared to unstrained tissue equivalent (left column).

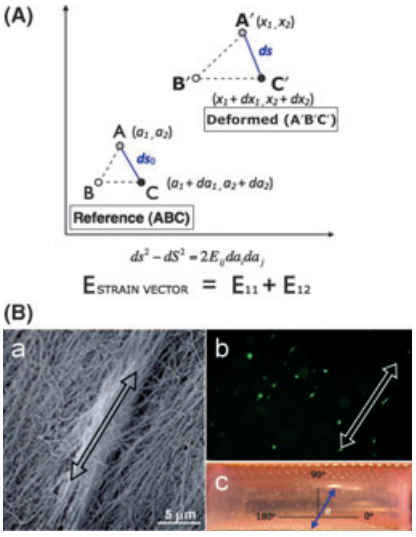

Fig. 6. Correlation of cell and fibre alignment with principal strain vector. (A) Strain calculation method using the position of a triad of markers in the reference (ABC) and deformed (A′B′C′) states. The strain is calculated by comparing the distance between the two markers A and C in the reference (ds_0) to the distance between the same two markers A′C′ in the deformed states (ds). (B) Orientation of cell (b) and fibres (a) in a strained cell-seeded tissue equivalent and direction of principal strain (c) in a shear stress system.

angle from the axis of titanium mesh displacement. The direction of cell and fibre alignment was compared to the principal strain angle (Fig. 6B).

Discussion

The present study showed that the ordered structure of the natural PDL was mimicked *in vitro* by applying shear stress to align collagen fibres and PDL cells within a three-dimensional tissue equivalent. Collagen fibres and cells aligned strongly in the direction of applied shear strain, as evidenced by the small angular deviation and the qualitative direction of fibre alignment in strained tissue equivalents. Shear stress was thought to be the most appropriate biomechanical stress for PDL tissue engineering because a tissue-specific stress could provide the enhanced functional competency in final tissue constructs for the tissues under physiological stress (Niklason et al. 1999, Akhyari et al. 2002, Waldman et al. 2004). It was demonstrated in our study that shear stress aligned PDL cells and collagen fibres with significantly higher uniformity.

The shear stress distribution in a three-dimensional collagen gel, determined by the finite element method showed that the centre of the shear stress system was homogenous in stress distribution throughout the entire thickness. The PDL cell-seeded tissue equivalent in our study showed the homogenous alignment of cells and collagen fibres along the principal strain vector under shear stress condition. Our alignment analysis in the shear stress system showed that PDL cells aligned in a direction parallel to their principal

strain vector. A cell in the system showed angular changes until it reached the direction of principal strain vector (Fig. 4A). No further changes were noted, because the cell was at its lowest strain energy state when situated in this direction of the principal strain vector. In other words, cells were aligned in a way that they react to minimize the perceived strain in their matrix (Eastwood et al. 1998).

Collagen fibres in the strained unseeded tissue equivalent aligned strongly in the direction of principle strain, as shown by the small angular deviation and the qualitative direction of the fibre alignment. Generally, the cellular involvement was shown to be a significant factor in collagen fibre alignment (Wang et al. 2003). In their *in vitro* experiment, if cells were randomly oriented, new collagen fibres produced by the cells were disorganized. On the other hand, if cells were aligned along a specific direction, collagen fibres laid down by cells showed alignment along the direction of the cells. This suggested that the orientation of cells dictated the alignment of collagen fibres produced by the cells. However, collagen fibres in our shear stress system are considered an existing matrix. Therefore, we showed that the collagen fibres were aligned in the absence of cells directly by an external mechanical cue. Similar findings were reported in studies including those using vertical shear flow (Kureshi et al. 2010), constrained gels (Thomopoulos et al. 2005) and uniaxial tensile loading (Kostyuk & Brown 2004). However, newly produced collagen fibres might require cellular involvement for their alignment.

Our quantitative analysis showed that shear stress aligned collagen fibres and PDL cells in a direction parallel to their principal strain vector. As was observed in Fig 4A, the cells in our shear stress system gradually oriented themselves along the directions of principal strain vectors at different time points. This implies that the collagen fibres, where cells reside, aligned along the same direction. Therefore, it is reasonable to expect that the change of direction of shear stress would result in an alignment change of cells and fibres along the direction of their new principal strain vector.

Unstrained tissue equivalents showed weak alignment of fibres and cells, characterized by the high angular deviation and the qualitative direction of fibre alignment, due to the uniaxial constraint imposed by the titanium meshes. Fibroblasts under static conditions have been observed to align both multidirectionally (Eastwood et al. 1998, Chiba & Mitani 2004) and unidirectionally (Costa et al. 2003). Fibres and cells aligned parallel to the free edges of the gel because strain was created when the tissue equivalent attempted to contract uniformly while being constrained in one dimension by the opposing titanium meshes. The change in angle of orientation and the increased order of collagen fibres in unstrained seeded tissue equivalents compared with unstrained unseeded tissue equivalents may be due to the presence of the cell traction force proposed by the anisotropic biphasic theory for tissue equivalent mechanics (Barocas & Tranquillo 1997). This theory supported our finding that the fibres in cell-seeded unstrained gels aligned parallel to the free edges of the gels with higher uniformity.

The three-dimensional tissue equivalent with a functional alignment of PDL cells and fibres induced by shear stress may have clinical implications for periodontal regeneration therapy. Flores et al. (2008) showed that transplantation of human PDL cell sheet into periodontal fenestration defects of immunodeficient rats induced periodontal regeneration with a new cementum and Sharpey's fibres. Gault et al. (2010) demonstrated that PDL cell-covered implants (ligaplants) inserted into a dog's alveolus could have a functional arrangement of cells and fibres in newly regenerated PDL-like tissues as well as cementum-like layers and alveolar bone-like tissues around the implants. The implants used in this canine model were coated with hydroxyapatites and fibronectin, suggesting that the implant surface was modified to induce cementogenesis or a formation of mineralized tissues that allowed a PDL to attach the surface of the implant for its functional arrangement. As an *in vitro* preparation for implantation shown in Flores et al. (2008) and Gault et al. (2010), a shear stress-induced PDL tissue construct with a functional orientation of PDL cells and fibres has a therapeutic advantage because the ordered structure of the construct could guide the arrangement of newly regenerated PDL and further provide the biomechanical stability for implanted teeth or artificial fixtures.

In conclusion, our study showed an *in vitro* technique to establish a functional alignment of collagen fibres and cells of the natural PDL by applying shear stress to a three-dimensional tissue equivalent seeded with PDL cells. The cell and fibre alignment of the engineered PDL was precisely guided by mechanical shear stress using a novel custom-designed bioreactor, suggesting that the enhanced functional property of engineered PDL constructs could be achieved with this technique.

Acknowledgements

We thank Dr. Songtao Shi for PDL cells, Dr. Xiaoxian Meng for statistical analysis, Nahn Ju Kim for rheology test and FFT analysis, Dr. Chang Lee and Dr. Charles Solomon for critiques.

Author contributions: S.G.K., S.-G. K., S.K., B.V. and H.-D.N. designed the study, S.G.K. and B.V. collected the data and S.G.K. B.V. and H.-D. N. wrote and edited the manuscript.

References

Akhyari, P., Fedak, P. W., Weisel, R. D., Lee, T.-Y., Verma, S., Mickle, D. A. & Li, R.-K. (2002) Mechanical stretch regimen enhances the formation of bioengineered autologous cardiac muscle grafts. *Circulation* **106**(12 Suppl. 1), I137–I142.

Barocas, V. H. & Tranquillo, R. T. (1997) An anisotropic biphasic theory of tissue equivalent mechanics: the interplay among cell traction, fibrillar network deformation, fibril alignment, and cell contact guidance. *Journal of Biomechanical Engineering* **119**, 137–145.

Beertsen, W. (1987) Collagen phagocytosis by fibroblasts in the periodontal ligament of the mouse molar during the initial phase of hypofunction. *Journal of Dental Research* **66**, 1708–1712.

Beertsen, W., McCulloch, C. A. & Sodek, J. (1997) The periodontal ligament: a unique, multifunctional connective tissue. *Periodontology 2000* **13**, 20–40.

Bernstein, A. B., Preisig, E. & Schroeder, H. E. (1988) Formation of a new fibrous attachment to human dental roots. A new vitro model for studying periodontal regeneration. *Cell and Tissue Research* **254**, 659–670.

Buser, D., Warrer, K. & Karring, T. (1990) Formation of a periodontal ligament around titanium implants. *Journal of Periodontology* **61**, 597–601.

Chiba, M. & Mitani, H. (2004) Cytoskeletal changes and the system of regulation of alkaline phosphatase activity in human periodontal ligament cells induced by mechanical stress. *Cell Biochemistry Function* **22**, 249–256.

Choi, B.-H. (2000) Periodontal ligament formation around titanium implants using cultured periodontal ligament cells: a pilot study. *International Journal of Oral and Maxillofacial Implants* **15**, 193–196.

Cohn, S. A. (1966) Disuse atrophy of the periodontium in mice following partial loss of function. *Archives of Oral Biology* **11**, 95–105.

Costa, K. D., Lee, E. J. & Holmes, J. W. (2003) Creating alignment and anisotropy in engineered heart tissue: role of boundary conditions in a model three dimensional culture system. *Tissue Engineering* **9**, 567–577.

Cronin, R. J. Jr, Oesterle, L. J. & Ranly, D. M. (1994) Mandibular implants and the growing patient. *International Journal of Oral Maxillofacial Implants* **9**, 55–62.

Eastwood, M., Mudera, V. C., McGrouther, D. A. & Brown, R. A. (1998) Effect of precise mechanical loading on fibroblast populated collagen lattices: morphological changes. *Cell Motility and Cytoskeleton* **40**, 13–21.

Flores, M. G., Yashiro, R., Washio, K., Yamato, M., Okano, T. & Ishikawa, I. (2008) Periodontal ligament cell sheet promotes periodontal regeneration in athymic rats. *Journal of Clinical Periodontology* **35**, 1066–10072.

Gault, P., Black, A., Romette, J.-L., Fuente, F., Schroeder, K., Thillou, F., Brune, T., Berdal, A. & Wurtz, T. (2010) Tissue-engineered ligament: implant constructs for tooth replacement. *Journal of Clinical Periodontology* **37**, 750–758.

Gray, J. L. & Vernino, A. R. (2004) The interface between retained roots and dental implants: a histologic study in baboons. *Journal of Periodontology* **75**, 1102–1106.

Henneman, S., Von den Hoff, J. W. & Maltha, J. C. (2008) Mechanobiology of tooth movement. *European Journal of Orthodontics* **30**, 299–306.

Hillmann, G., Gebert, A. & Geurtsen, W. (1999) Matrix expression and proliferation of primary gingival fibroblasts in a three-dimensional cell culture model. *Journal of Cell Science* **112**, 2823–2832.

Kostyuk, O. & Brown, R. A. (2004) Novel spectroscopic technique for *in situ* monitoring of collagen fibril alignment in gels. *Biophysical Journal* **87**, 648–655.

Kureshi, A., Cheema, U., Alekseeva, T., Cambrey, A. & Brown, R. (2010) Alignment hierarchies: engineering architecture from the nanometre to the micrometre scale. *Journal of the Royal Society Interface* **7**(Suppl. 6), S707–S716.

Levy, G. G. & Mailland, M. L. (1980) Histologic study of the effects of occlusal hypofunction following antagonist tooth extraction in the rat. *Journal of Periodontology* **51**, 393–399.

Niklason, L. E., Gao, J., Abbott, W. M., Hirschi, K. K., Houser, S., Marini, R. & Langer, R. (1999) Functional arteries grown *in vitro*. *Science* **284**, 489–493.

Parlar, A., Bosshardt, D. D., Unsal, B., Cetiner, D., Haytac, C. & Lang, N. P. (2005) New formation of periodontal tissues around titanium implants in a novel dentin chamber model. *Clinical Oral Implants Research* **16**, 259–267.

Preisig, E. & Schroeder, H. E. (1988) Long-term culture of human periodontal ligament cells with autologous root discs. *Journal of Periodontal Research* **23**, 211–221.

Roeder, B. A., Kokini, K., Robinson, J. P. & Voytik-Harbin, S. L. (2004) Local, three-dimensional strain measurements within largely deformed extracellular matrix constructs. *Journal of Biomechanical Engineering* **126**, 699–708.

Seo, B.-M., Miura, M., Gronthos, S., Bartold, P. M., Batouli, S., Brahim, J., Robey, P. G., Wang, C. Y. & Shi, S. (2004) Investigation of multipotent postnatal stem cells from human periodontal ligament. *Lancet* **364**, 149–155.

Thomopoulos, S., Fomovsky, G. M. & Holmes, J. W. (2005) The development of structural and mechanical anisotropy in fibroblast populated collagen gels. *Journal of Biomechanical Engineering* **127**, 742–750.

Wagenseil, J. E., Elson, E. L. & Okamoto, R. J. (2004) Cell orientation influences the biaxial mechanical properties of fibroblast populated collagen vessels. *Annals of Biomedical Engineering* **32**, 720–731.

Waldman, S. D., Spiteri, C. G., Grynpas, M. D., Pilliar, R. M. & Kandel, R. A. (2004) Long-term intermittent compressive stimulation improves the composition and mechanical properties of tissue engineered cartilage. *Tissue Engineering* **10**, 1323–1331.

Wang, J. H., Jia, F., Gilbert, T. W. & Woo, S. L. (2003) Cell orientation determines the alignment of cell-produced collagenous matrix. *Journal of Biomechanics* **36**, 97–102.

Warrer, K., Karring, T. & Gotfredsen, K. (1993) Periodontal ligament formation around different types of dental titanium implants. I. The self-tapping screw type implant system. *Journal of Periodontology* **64**, 29–34.

Young, C. S., Abukawa, H., Asrican, R., Ravens, M., Troulis, M. J., Kaban, L. B., Vacanti, J. P. & Yelick, P. C. (2005) Tissue engineered hybrid tooth and bone. *Tissue Engineering* **11**, 1599–1610.

Address:
S. G. Kim
Division of Endodontics
College of Dental Medicine
Columbia University
630 W 168th Street
PH7Stem
New York
NY 10032
USA
E-mail: sgk2114@columbia.edu

Clinical Relevance

Scientific rationale for the study: An engineered PDL tissue construct mimics the natural PDL.
Principal findings: A functional alignment of collagen fibres and cells of the natural PDL was established by applying shear stress to a three-dimensional tissue equivalent seeded with PDL cells. The alignment of cells and fibres could be guided by mechanical shear stress using a custom-designed bioreactor.
Practical implications: An engineered PDL tissue construct with a functional alignment of PDL cells and collagen fibres may have enhanced functional properties when it was implanted *in vivo* with a regenerated tooth or a dental implant.